Molecular Therapy
Nucleic Acids
Original Article

Long Noncoding RNA OIP5-AS1 Promotes the Progression of Liver Hepatocellular Carcinoma via Regulating the hsa-miR-26a-3p/EPHA2 Axis

Yu-Shui Ma,[1,2,7] Kai-Jian Chu,[3,7] Chang-Chun Ling,[4,7] Ting-Miao Wu,[5,7] Xu-Chao Zhu,[2] Ji-Bin Liu,[6] Fei Yu,[2] Zhi-Zhen Li,[3] Jing-Han Wang,[3] Qing-Xiang Gao,[3] Bin Yi,[3] Hui-Min Wang,[2] Li-Peng Gu,[2] Liu Li,[2] Lin-Lin Tian,[2] Yi Shi,[2] Xiao-Qing Jiang,[3] Da Fu,[2,5] and Xiong-Wen Zhang[1]

[1]Shanghai Engineering Research Center of Molecular Therapeutics and New Drug Development, College of Chemistry and Molecular Engineering, East China Normal University, Shanghai 200062, China; [2]Central Laboratory for Medical Research, Shanghai Tenth People's Hospital, Tongji University School of Medicine, Shanghai 200072, China; [3]Department of Biliary Tract Surgery I, Eastern Hepatobiliary Surgery Hospital, Shanghai 200438, China; [4]Department of General Surgery, The Affiliated Hospital of Nantong University, Nantong 226001, Jiangsu Province, China; [5]Department of Radiology, The Forth Affiliated Hospital of Anhui Medical University, Hefei 230012, China; [6]Cancer Institute, Nantong Tumor Hospital, Nantong 226631, China

Numerous studies have suggested that dysregulated long noncoding RNAs (lncRNAs) contributed to the development and progression of many cancers. lncRNA OIP5 antisense RNA 1 (OIP5-AS1) has been reported to be increased in several cancers. However, the roles of OIP5-AS1 in liver hepatocellular carcinoma (LIHC) remain to be investigated. In this study, we demonstrated that OIP5-AS1 was upregulated in LIHC tissue specimens and its overexpression was associated with the poor survival of patients with LIHC. Furthermore, loss-of function experiments indicated that OIP5-AS1 promoted cell proliferation and inhibited cell apoptosis both *in vitro* and *in vivo*. Moreover, binding sites between OIP5-AS1 and hsa-miR-26a-3p as well as between hsa-miR-26a-3p and EPHA2 were confirmed by luciferase assays. Finally, a rescue assay was performed to prove the effect of the OIP5-AS1/hsa-miR-26a-3p/EPHA2 axis on LIHC cell biological behaviors. Based on all of the above findings, our results suggested that OIP5-AS1 promoted LIHC cell proliferation and invasion via regulating the hsa-miR-26a-3p/EPHA2 axis.

INTRODUCTION

Liver hepatocellular carcinoma (LIHC) is one of the most common causes of cancer-related mortality in the world.[1–3] About 80% of LIHC patients have lost the chance of operation because of the occult onset and rapid progress.[4–6] At present, all kinds of treatments for LIHC can delay the progress of LIHC, but they cannot significantly improve the survival period of LIHC patients in the middle and late stage.[7–9] Therefore, it is urgent to study the molecular mechanism of LIHC, determine the biomarkers and treatment targets for disease diagnosis, and seek new treatment plans to improve the prognosis.

Noncoding RNAs (ncRNAs) are new kinds of transcripts encoded by the genome, but most of them are not translated into proteins.[10–13] Although not translated, ncRNA performs various cellular and physiological functions. In particular, long noncoding RNA (lncRNA, ncRNA longer than 200 nt) regulates chromatin dynamics, gene expression, growth, differentiation, and development.[14–17] In addition to mutations or aberrant expression in the protein-coding genes, mutations and misregulation of ncRNAs, in particular lncRNA, appear to play major roles in cancer.[18–20] Much evidence shows that lncRNA is involved in many biological processes, such as cancer cell proliferation, apoptosis, invasion, and so on.[21–26] Moreover, because of their genome-wide expression patterns in a variety of tissues and their tissue specific expression characteristics, lncRNAs hold strong promise as novel biomarkers and therapeutic targets for cancer.[27–30]

lncRNA OIP5 antisense RNA 1 (OIP5-AS1), a prominent tumor-associated lncRNA, contributes to intricate cellular mechanisms during tumorigenesis and development of malignant tumors.[31–35] For example, it not only represses cyclin G-associated kinase (GAK) expression, thus impacting mitosis, but it also regulates proliferation, metastasis, and epithelial-to-mesenchymal transition (EMT) progress and apoptosis in many cancers, including lung adenocarcinoma, breast cancer, glioma, multiple myeloma, and colorectal cancer.[36–40]

However, its specific mechanism and role in LIHC remains to be fully elucidated. The purpose of this study is to reveal that the abnormal expression of lncRNA is closely related to the occurrence and development of tumors, to explore the biological function of lncRNA and its regulatory mechanism in liver cancer, so as to understand the

Received 20 February 2020; accepted 28 May 2020;
https://doi.org/10.1016/j.omtn.2020.05.032.

[7]These authors contributed equally to this work.

Correspondence: Da Fu, Central Laboratory for Medical Research, Shanghai Tenth People's Hospital, Tongji University School of Medicine, Shanghai 200072, China.
E-mail: fu800da900@126.com
Correspondence: Xiong-Wen Zhang, Shanghai Engineering Research Center of Molecular Therapeutics and New Drug Development, College of Chemistry and Molecular Engineering, East China Normal University, Shanghai 200062, China.
E-mail: xwzhang@sat.ecnu.edu.cn

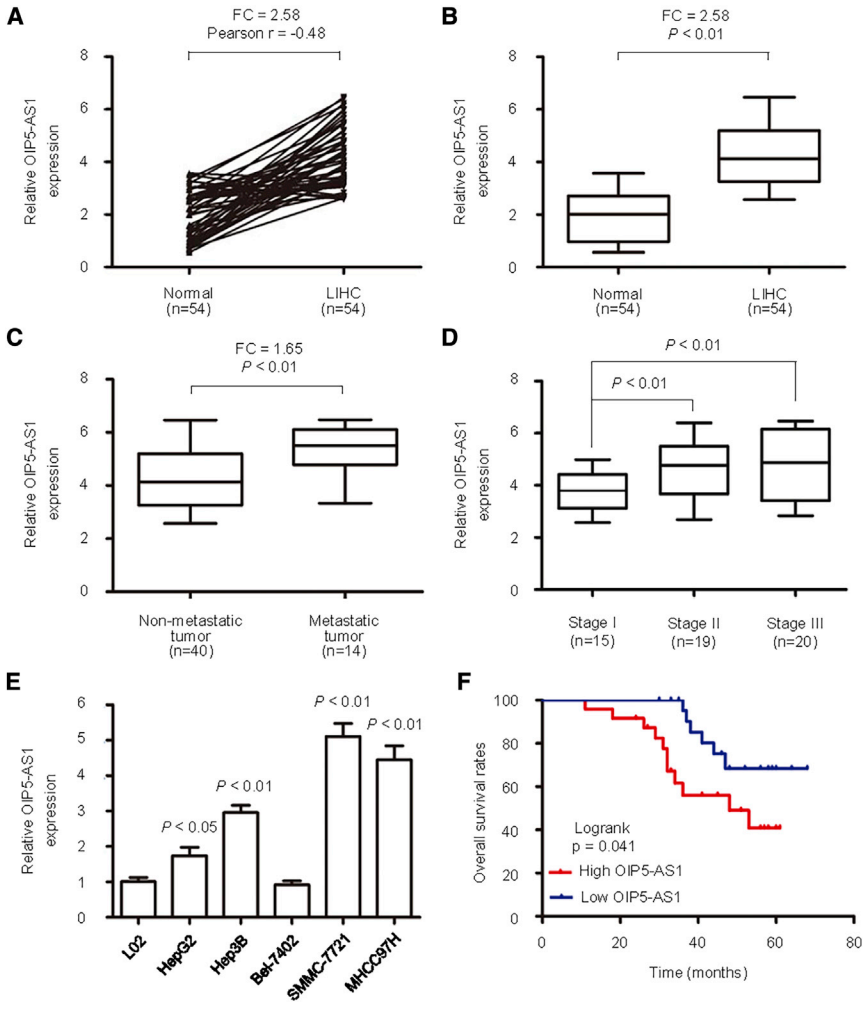

Figure 1. The Expression of OIP5-AS1 Was High in LIHC Samples and Cell Lines

(A and B) The expression level (A) and correlation (B) of OIP5-AS1 in 54 pairs of LIHC tissues and adjacent noncancerous tissues were identified using quantitative real-time PCR. (C) Relative levels of OIP5-AS1 in patients with metastasis or without metastasis. (D) Expression levels of OIP5-AS1 in different stages are shown. (E) OIP5-AS1 expression level was examined in LIHC cell lines and a normal live cell line. (F) The Kaplan-Meier method was used to evaluate the relationship between OIP5-AS1 expression and overall survival of LIHC patients.

pathogenesis of diseases more comprehensively, and to find new diagnostic markers of diseases, as well as therapeutic targets, and provide new ideas and methods for treatment.

RESULTS

Identification of Significantly Dysregulated lncRNAs in LIHC

Analysis from The Cancer Genome Atlas (TCGA) sequencing dataset identified a total of 5,326 significantly changed lncRNAs in LIHC, with the cutoff point of $\geq$2-fold changes (FCs) for upregulated lncRNAs and $\leq$0.5-FCs for downregulated lncRNAs. A total of 25 genes were extremely significantly changed ($p < 1E{-}40$) in the tumor tissues group compared to the adjacent non-tumor tissues from LIHC patients, of which 23 were upregulated and 2 were downregulated (Figure S1A).

Subsequently, Kaplan-Meier survival curves were plotted to estimate the prognostic value of 25 extremely significantly changed lncRNAs in LIHC. We recorded lncRNA expression level as high versus low using a cutoff point of the median. Univariate analysis of overall survival (OS) by Kaplan-Meier survival analysis indicated that high lncRNA CRNDE ($p = 0.048$; Figure S1B), OIP5-AS1 ($p = 0.032$; Figure S1C), or ZEB1-AS1 ($p = 0.028$; Figure S1D) expression was associated with shorter OS in 371 LIHC patients.

In 371 LIHC samples, there was more CRNDE (FC = 9.61, p = 1.43E−41; Figure S2A), OIP5-AS1 (FC = 1.53, p = 3.54E−42; Figure S2B), and ZEB1-AS1 (FC = 2.93, p = 1.06E−44; Figure S2C) expression when compared to non-tumor samples. In addition, in 50 pairs of LIHC samples and adjacent normal liver samples, the expression values of CRNDE (FC = 12.57, Pearson r = −0.12; Figure S2D), OIP5-AS1 (FC = 2.14, Pearson r = −0.68; Figure S2E), and ZEB1-AS1 (FC = 3.22, Pearson r = −0.25; Figure S2E) in non-tumoral adjacent tissues and LIHC tissues were significantly negatively correlated.

Next, we evaluated the expression of CRNDE, OIP5-AS1, and ZEB1-AS1 expression levels in the Gene Expression Omnibus (GEO) database and only found upregulated OIP5-AS1 expression in GEO: GSE104310 (FC = 2.56, p = 0.019; Figure S2G). We then validated the aforementioned findings in another set of 38 paired LIHC versus non-cancerous tissue samples. GEO: GSE84005 data also demonstrated that the OIP5-AS1 level was significantly enhanced in LIHC samples compared with that in normal controls (FC = 2.21, p = 0.003; Figure S2H). Furthermore, analysis of 371 LIHC samples from TCGA sequencing dataset identified significant correlation between OIP5-AS1 expression and tumor stage (Figure S2I).

lncRNA OIP5-AS1 Is Upregulated in LIHC Tissues and Cell Lines

The expression of OIP5-AS1 was detected by quantitative real-time PCR in 54 cases of liver cancer and six cell lines. The results showed that the expression of OIP5-AS1 in LIHC was significantly higher than that in adjacent tissues (Figures 1A and 1B). Compared with non-metastatic LIHC, the expression level of OIP5-AS1 in metastatic LIHC was significantly upregulated (Figure 1C), and the high expression was significantly related to tumor stage ($p < 0.01$; Figure 1D). The expression of OIP5-AS1 in HepG2, Hep3B, SMMC-7721, and

MHCC97H cells was significantly higher than that in L02 cells, and the highest expression was found in SMMC-7721 cells ($p < 0.05$; Figure 1E). The expression levels of OIP5-AS1 in HepG2, Hep3B, SMMC-7721, and MHCC97H cells were significantly higher than that of L02 cells ($p < 0.05$). Moreover, a Kaplan-Meier survival curve showed that in newly diagnosed patients with liver cancer, the OS of patients with high expression of OIP5-AS1 was significantly shortened (Figure 1F).

Knockdown of OIP5-AS1 Inhibits Cell Proliferation and Invasion *In Vitro*

In order to evaluate the effect of inhibiting the expression of OIP5-AS1 on the proliferation, apoptosis, and invasiveness of SMMC-7721 and MHCC97H cells, stable knockdown cell lines were obtained by short hairpin RNA (shRNA) interference with OIP5-AS1, and the expression of OIP5-AS1 in SMMC-7721 and MHCC97H cell lines was detected by quantitative real-time PCR, which confirmed that the expression level of OIP5-AS1 was significantly reduced (Figures 2A and 2B). The results showed that compared with Random shRNA sequence control (SCR), the growth rate of the shRNA1 and shRNA2 groups decreased significantly ($p < 0.05$) in SMMC-7721 (Figure 2C) and MHCC97H (Figure 2D) cell lines. The apoptosis analysis in the shRNA1, shRNA2, and SCR groups was performed by flow cytometry, and the results showed that compared with the SCR group, the apoptosis of the shRNA1 and shRNA2 groups significantly increased (1.00 ± 0.06, $p < 0.05$) (Figure 2E). Transwell experimental analysis showed that the invasiveness of SMMC-7721 and MHCC97H cells after OIP5-AS1 shRNA was weaker than that in the SCR group (1.00 ± 0.06, $p < 0.05$) (Figure 2F).

OIP5-AS1 Is a Molecular Sponge Regulating hsa-miR-26a-3p

In order to study the role of OIP5-AS1 in the carcinogenesis and development of liver cancer and the downstream regulated genes, we predicted the target through starBase 2.0 and found that the 3′ UTR of OIP5-AS1 matched the "seed sequence" of hsa-miR-26a-3p (Figure 3A). In order to verify whether OIP5-AS1 is the direct target of hsa-miR-26a-3p in hepatoma cells, we carried out a luciferase reporter gene assay to confirm that hsa-miR-26a-3p can combine with the 3′ UTR of OIP5-AS1. The results showed that the increased hsa-miR-26a-3p significantly inhibited the luciferase activity of wild-type (WT) OIP5-AS1 3′ UTR, but it had no effect on mutant (MT) 3′ UTR; on the contrary, the decreased hsa-miR-26a-3p increased the luciferase activity of WT OIP5-AS1 3′ UTR, but it did not affect the luciferase activity of MT OIP5-AS1 3′ UTR (Figure 3B). By inhibiting OIP5-AS1 in SMMC-7721 and MHCC97H cells, the expression of hsa-miR-26a-3p mRNA increased significantly ($p < 0.05$, Figure 3C). Thus, OIP5-AS1 is a molecular sponge regulating hsa-miR-26a-3p.

Next, we detected the expression of hsa-miR-26a-3p in 54 paired LIHC and adjacent normal liver tissues. The data showed that the level of hsa-miR-26a-3p in liver cancer was significantly lower than that in adjacent normal liver tissues ($p < 0.05$, Figure 3D). Spearman correlation analysis showed that the expression of OIP5-AS1 was negatively correlated with that of hsa-miR-26a-3p ($n = 54$, $R^2 = 0.47$, $p < 0.001$; Figure 3E).

Evaluation of Expression and Prognostic Value of hsa-miR-26a-3p in LIHC Patients

We evaluated the expression of hsa-miR-26a-3p in TCGA sequencing dataset and found the lower hsa-miR-26a-3p expression in tumor tissues compared to the adjacent non-tumor tissues from LIHC patients (FC = 0.46, p = 1.24E−08; Figure S3A). In 50 pairs of LIHC samples and adjacent normal liver samples, the expression values of hsa-miR-26a-3p in non-tumoral adjacent tissues and LIHC tissues were 10.85 ± 0.96 and 4.45 ± 0.12, respectively (FC = 0.41, p = 5.65E−25; Figure S3B). The expression values of hsa-miR-26a-3p in non-tumoral adjacent tissues and LIHC tissues were significantly negatively correlated (Pearson r = −0.25, p = 0.0048; Figure S3C). Furthermore, analysis of 371 LIHC samples from TCGA sequencing dataset identified significant correlation between hsa-miR-26a-3p expression and tumor stage (Figure S3D). Low hsa-miR-26a-3p expression was associated with shorter OS in LIHC patients (p = 0.036; Figure S3E). Kaplan-Meier analysis of OS indicated that low hsa-miR-26a-3p expression together with high OIP5-AS1 level were correlated with a worse OS (p = 0.002; Figure S3F).

Next, we evaluated the correlation of hsa-miR-26a-3p and OIP5-AS1 expression levels and found a significant negative correlation between hsa-miR-26a-3p and OIP5-AS1 expression in 50 normal liver samples (Pearson r = −0.38, p = 0.042; Figure S3G) and in 371 LIHC samples (Pearson r = −0.42, p = 3.68E−4; Figure S3H). We then validated the aforementioned findings in a GEO set. GEO: GSE21362 data demonstrated that the hsa-miR-26a-3p level was significantly downregulated in LIHC samples compared with that in normal controls (FC = 0.52, $p < 0.001$; Figure S3I). Data from GEO: GSE36915 also demonstrated a decreased level of hsa-miR-26a-3p expression in LIHC samples compared with that in normal controls (FC = 0.33, $p < 0.001$; Figure S3J).

Furthermore, analysis of 241 LIHC samples from the GEO: GSE6857 dataset identified that hsa-miR-26a-3p expression was lower in metastatic LIHC tissues compared with non-metastatic LIHC tissues (FC = 0.55, $p < 0.0001$) or normal tissues (FC = 0.76, $p < 0.01$) (Figure S3K). Furthermore, LIHC samples from living (n = 178) and deceased (n = 59) patients were screened for hsa-miR-26a-3p expression, with expression values of 7.85 ± 0.89 and 3.29 ± 0.33, respectively (FC = 0.42, $p < 0.0001$; Figure S3L).

lncRNA OIP5-AS1 Negatively Regulated hsa-miR-26a-3p to Accelerate Cell Proliferation and Invasion in LIHC

In order to further study the relationship between OIP5-AS1 and hsa-miR-26a-3p *in vitro*, we transfected anti-hsa-miR-26a-3p in SMMC-7721 and MHCC97H cells with OIP5-AS1 shRNA. When compared with the anti-miR-negative control (NC) group, the expression of hsa-miR-26a-3p in the anti-hsa-miR-26a-3p group decreased significantly (0.97 ± 0.11 versus 12.15 ± 1.48, $p < 0.05$; Figure 4A). After knockdown of hsa-miR-26a-3p, the optical density (OD) value of cells

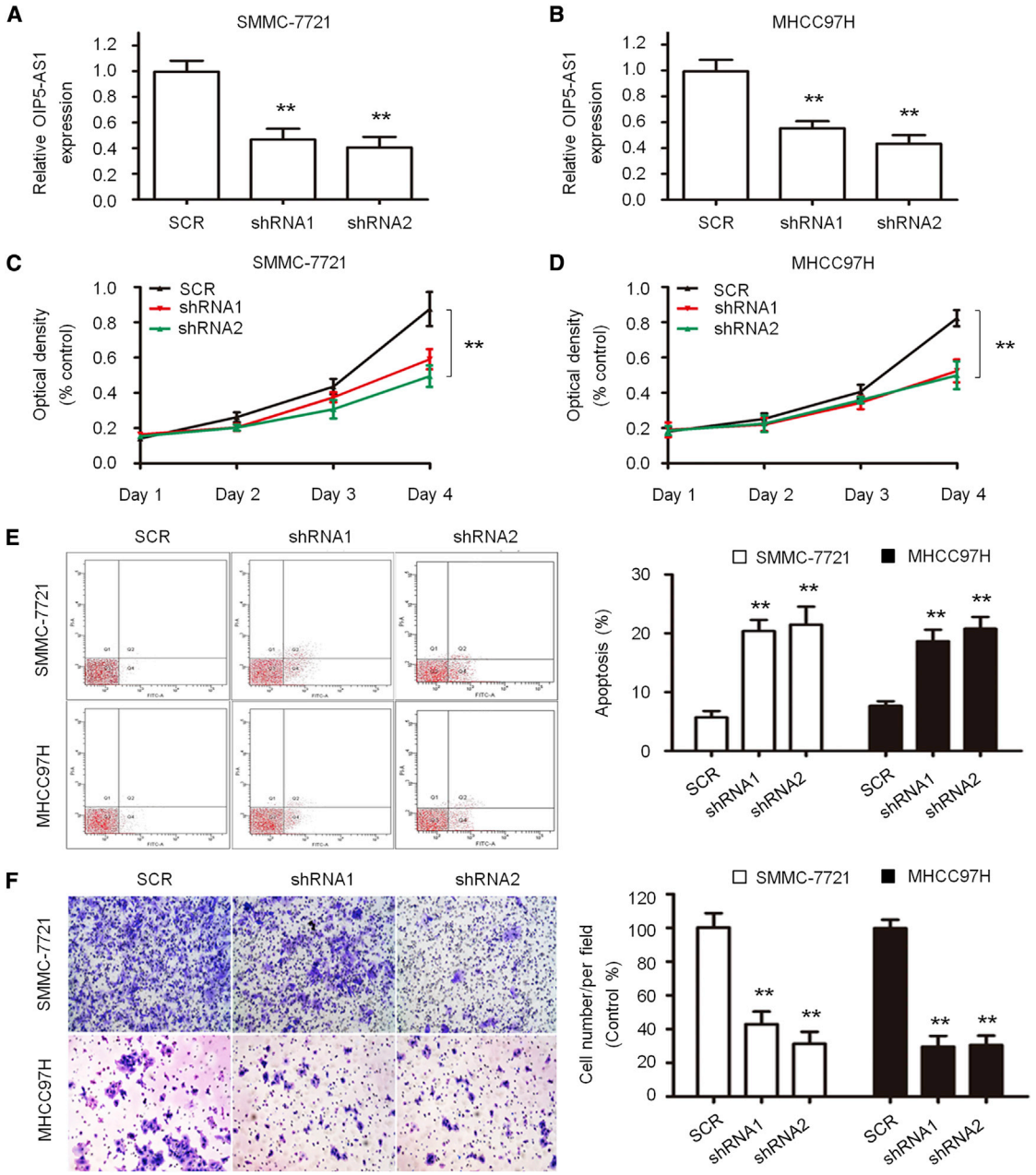

Figure 2. Effects of OIP5-AS1 on LIHC Cell Proliferation and Apoptosis

(A and B) Knockdown of OIP5-AS1 in SMMC-7721 (A) and MHCC97H (B) cells was confirmed by quantitative real-time PCR. (C and D) Viabilities of SMMC-7721 (C) and MHCC97H (D) cells were evaluated by a CCK-8 assay. (E) Cell apoptosis was assessed in SMMC-7721 and MHCC97H cells after OIP5-AS1 silencing by flow cytometry analysis. (F) Invasion of SMMC-7721 and MHCC97H cells was detected by a transwell invasion assay. **$p < 0.01$.

was significantly higher than that of the anti-miR-NC group (1.03 ± 0.10 versus 0.21 ± 0.03, $p < 0.05$; Figure 4B). By flow cytometry analysis, compared with the shRNA2 + anti-miR-NC group, the number of apoptotic cells in SMMC-7721 and MHCC97H cells in the shRNA2 + anti-hsa-miR-26a-3p group decreased significantly (1.00 ± 0.06, $p < 0.05$) (Figure 4C). Furthermore, the invasiveness of SMMC-7721 and MHCC97H cells in the shRNA2 + anti hsa-miR-26a-3p group was significantly enhanced compared with that in the shRNA2 + anti-miR-NC group (1.00 ± 0.06, $p < 0.05$) (Figure 4D). Thus, our data showed that the inhibition of hsa-miR-26a-3p partially eliminated the role of OIP5-AS1, resulting in the significant increase of proliferation, invasion, and inhibition of apoptosis in SMMC-7721 and MHCC97H cells inhibited by OIP5-AS1, suggesting that the change of hsa-miR-26a-3p partially promoted the

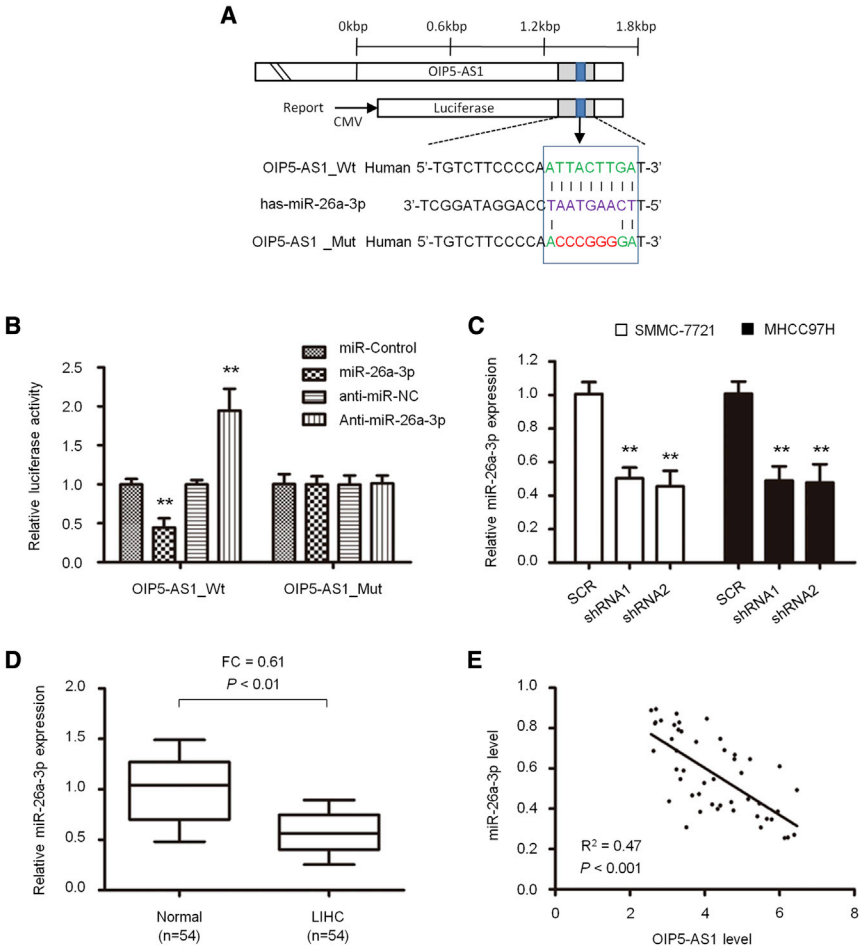

Figure 3. Interaction between OIP5-AS1 and hsa-miR-26a-3p in LIHC

(A) Sequence of the hsa-miR-26a-3p-binding site within the OIP5-AS1 predicted with starBase 2.0. Mutation was generated on the OIP5-AS1 in the complementary site for the seed region of hsa-miR-26a-3p. (B) Luciferase reporter assay was performed to detect the interaction between OIP5-AS1 with hsa-miR-26a-3p in HEK293T cells. (C) Expression of hsa-miR-26a-3p upon OIP5-AS1 silencing in LIHC cells was detected by quantitative real-time PCR. (D) hsa-miR-26a-3p expression in 54 pairs of LIHC tissues and adjacent noncancerous tissues. (E) Pearson's correlation curve showed the negative relationship between OIP5-AS1 and hsa-miR-26a-3p in LIHC tissues. **p < 0.01.

proliferation, invasion, and inhibition of apoptosis of hepatoma cells mediated by OIP5-AS1.

lncRNA OIP5-AS1 Acts as a Competing Endogenous RNA (ceRNA) for hsa-miR-26a-3p to Modulate EPHA2 Expression in LIHC cells

In order to explore the mechanism of hsa-miR-26a-3p in the progression of liver cancer, we next searched for the candidate targets of hsa-miR-26a-3p on TargetScan and found that the 3′ UTR of EPHA2 matched the seed sequence of hsa-miR-26a-3p (Figure 5A). In order to verify whether EPHA2 is a direct target of hsa-miR-26a-3p in hepatoma cells, we carried out a luciferase reporter gene assay to confirm that hsa-miR-26a-3p can bind to the 3′ UTR of EPHA2. The analysis showed that the increased hsa-miR-26a-3p significantly inhibited the luciferase activity of WT EPHA2 3′ UTR, but it had no effect on the MT EPHA2 3′-UTR; on the contrary, the decrease of hsa-miR-26a-3p increased the luciferase activity of WT EPHA2 3′ UTR, but it did not affect the luciferase activity of MT EPHA2 3′ UTR (Figure 5B). By overexpression of hsa-miR-26a-3p in SMMC-7721 and MHCC97H cells, the expression of EPHA2 mRNA (Figure 5C) and protein (Figure 5D) was significantly lower than that in the control group.

Next, we detected the expression of EPHA2 in LIHC and paracancerous tissues. The data showed that the level of EPHA2 in LIHC was significantly higher than that in paracancerous tissues ($p < 0.05$; Figure 5E). Spearman correlation analysis showed that OIP5-AS1 expression was negatively correlated with hsa-miR-26a-3p expression ($n = 54$, $R^2 = 0.41$; Figure 5F). In order to clarify the relationship between OIP5-AS1, hsa-miR-26a-3p, and EPHA2, we detected the expression of EPHA2 in MHCC97H and MHCC97H cells with shRNA-interfering OIP5-AS1 by quantitative real-time PCR and western blot (WB) and found that the expression level of EPHA2 mRNA (Figure 5G) and protein (Figure 5H) decreased significantly. Besides, the enrichment of OIP5-AS1, miR-26a-3p, and EPHA2 mRNA was all easily observed in anti-Ago2-induced immunoprecipitations (Figures 5I and 5J), suggesting the co-existence of the above three molecules in RNA-induced silencing complex. These results indicate that EPHA2 is the downstream protein of hsa-miR-26a-3p in LIHC.

Then, after knockdown of hsa-miR-26a-3p in MHCC97H and MHCC97H cells, in which shRNA interfered with OIP5-AS1, we detected the expression of EPHA2 protein by WB and confirmed the high level of EPHA2 protein expression (Figure 5K). In addition, Spearman correlation analysis showed that the expression of EPHA2 was positively correlated with that of OIP5-AS1 ($n = 54$, $R^2 = 0.29$; Figure 5L). Therefore, lncRNAOIP5-AS1 may enhance the function of EPHA2, promote cell proliferation, enhance cell invasion, and inhibit apoptosis by negatively regulating hsa-miR-26a-3p.

Knockdown of lncRNA OIP5-AS1 Inhibits Tumorigenesis *In Vivo*

In order to further confirm the significance of OIP5-AS1 function *in vivo*, we established a subcutaneous tumor model. The tumor growth curve showed that the interference of OIP5-AS1 with shRNA significantly inhibited tumor growth (Figures 6A and 6C) and tumor weight (Figure 6D). We detected the expression of hsa-miR-26a-3p in

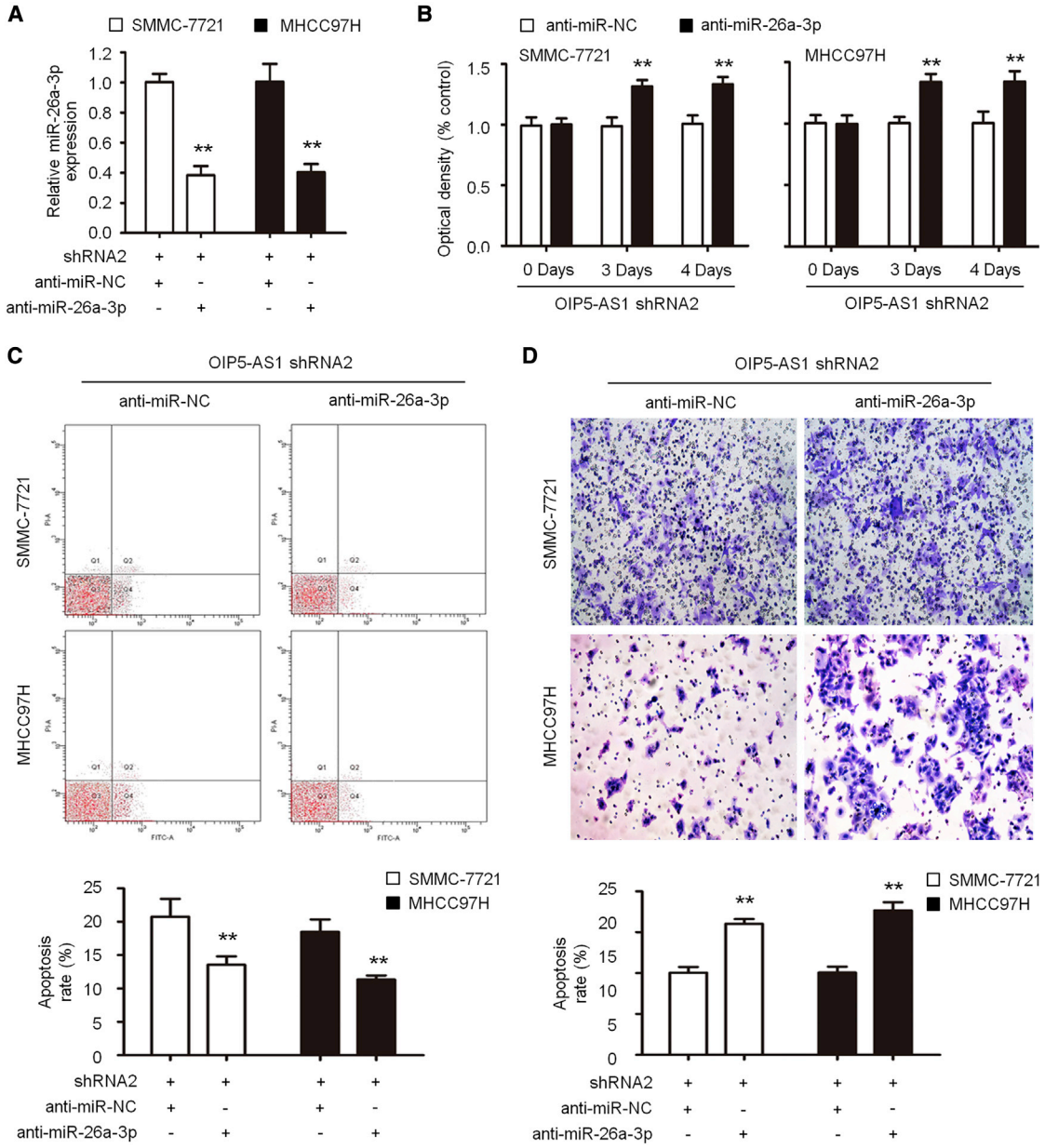

Figure 4. Knockdown of hsa-miR-26a-3p Partially Reversed the Tumor Suppressor Role of OIP5-AS1 Silencing in LIHC

(A) The expression of hsa-miR-26a-3p was decreased in cells co-transfected with sh-OIP5-AS1 and anti-hsa-miR-26a-3p compared with those only transfected with sh-OIP5-AS1. (B–D) Cell proliferation (B), apoptosis (C), and invasion (D) were determined as indicated. **p < 0.01.

MHCC97H cells, in which shRNA interfered with OIP5-AS1, by quantitative real-time PCR and found that the expression level of hsa-miR-26a-3p was significantly increased (Figure 6E). However, the levels of EPHA2 mRNA (Figure 6F) and protein levels (Figure 6G) were significantly increased. Next, we stained the slice from subcutaneous tumor with Ki67 and found that the knockdown of OIP5-AS1 significantly reduced the number of Ki67-positive cells (Figure 6H), suggesting that knockdown of OIP5-AS1 results in a significant decrease in the number of proliferation cells stained with Ki67.

DISCUSSION

Liver cancer is one of the most common causes of cancer-related mortality in the world.[41] Hepatocellular carcinoma accounts for the vast majority of all LIHC cases. Due to the occult onset and rapid progress of LIHC, 80% of the patients had lost the chance of operation.[42] Palliative resection, radiofrequency ablation, transarterial chemoembolization (TACE), systemic chemotherapy, and traditional Chinese medicine treatment can alleviate the symptoms of patients and delay the progress of LIHC, but they cannot

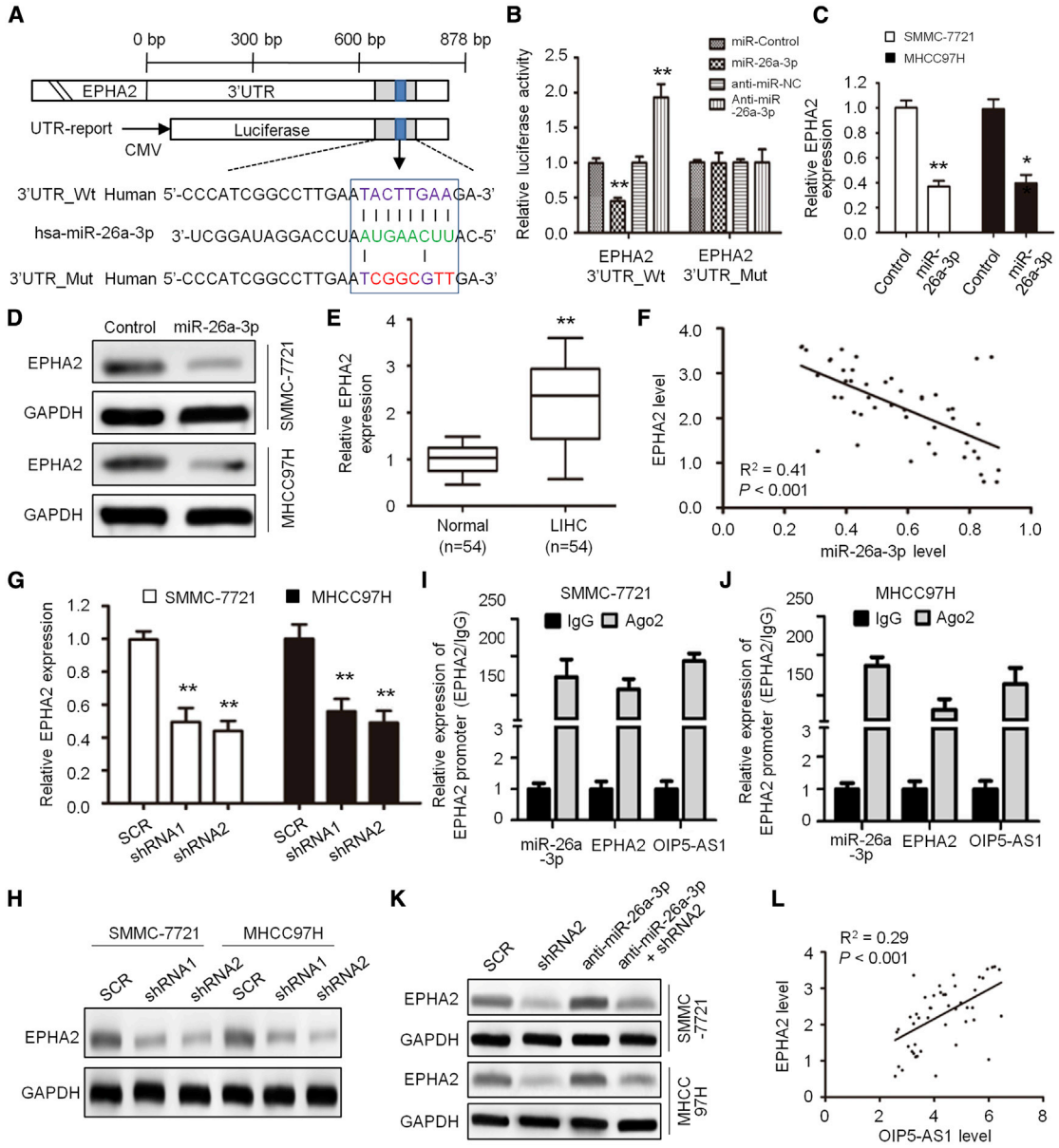

Figure 5. OIP5-AS1 Promotes EPHA2 Expression by Regulating hsa-miR-26a-3p

(A) Schematic representation of the hsa-miR-26a-3p binding sites in EPHA2 and the site mutagenesis. (B) Luciferase activity in HEK293T cells co-transfected with hsa-miR-26a-3p mimics or hsa-miR-26a-3p inhibitors and luciferase reporter plasmids containing wild-type EPHA2 or mutant EPHA2. (C and D) EPHA2 mRNA (C) and protein (D) levels in SMMC-7721 and MHCC97H cells following has-miR-26a-3p overexpression. (E) Relative mRNA expression levels of EPHA2 in 54 pairs of LIHC tissues and adjacent noncancerous tissues. (F) Pearson's correlation curve shows the negative relationship between OIP5-AS1 and hsa-miR-26a-3p in LIHC tissues. (G and H) EPHA2 mRNA (G) and protein (H) levels in SMMC-7721 and MHCC97H cells after OIP5-AS1 silencing. (I and J) The interaction of OIP5-AS1, miR-26a-3p, and EPHA2 mRNA was proved by RNA immunoprecipitation (RIP) assays in SMMC-7721 (I) and MHCC97H cells (J). (K) Protein expression of EPHA2 measured using western blot analysis as indicated. (L) Pearson's correlation curve shows the positive relationship between OIP5-AS1 and EPHA2 in LIHC tissues. **p < 0.01.

significantly improve the survival period of patients with advanced LIHC, which brings severe mental pressure and economic burden to patients.[43–46] Therefore, it is urgent to study the molecular mechanism of LIHC occurrence and determine the biomarkers for disease diagnosis.

Much evidence shows that lncRNA plays an important role in the proliferation, apoptosis, invasion, migration, and metastasis of cancer cells, and it also plays an important role in the occurrence and development of cancer.[47–49] At present, it has been found that there are significant differences in the expression of various lncRNAs in different

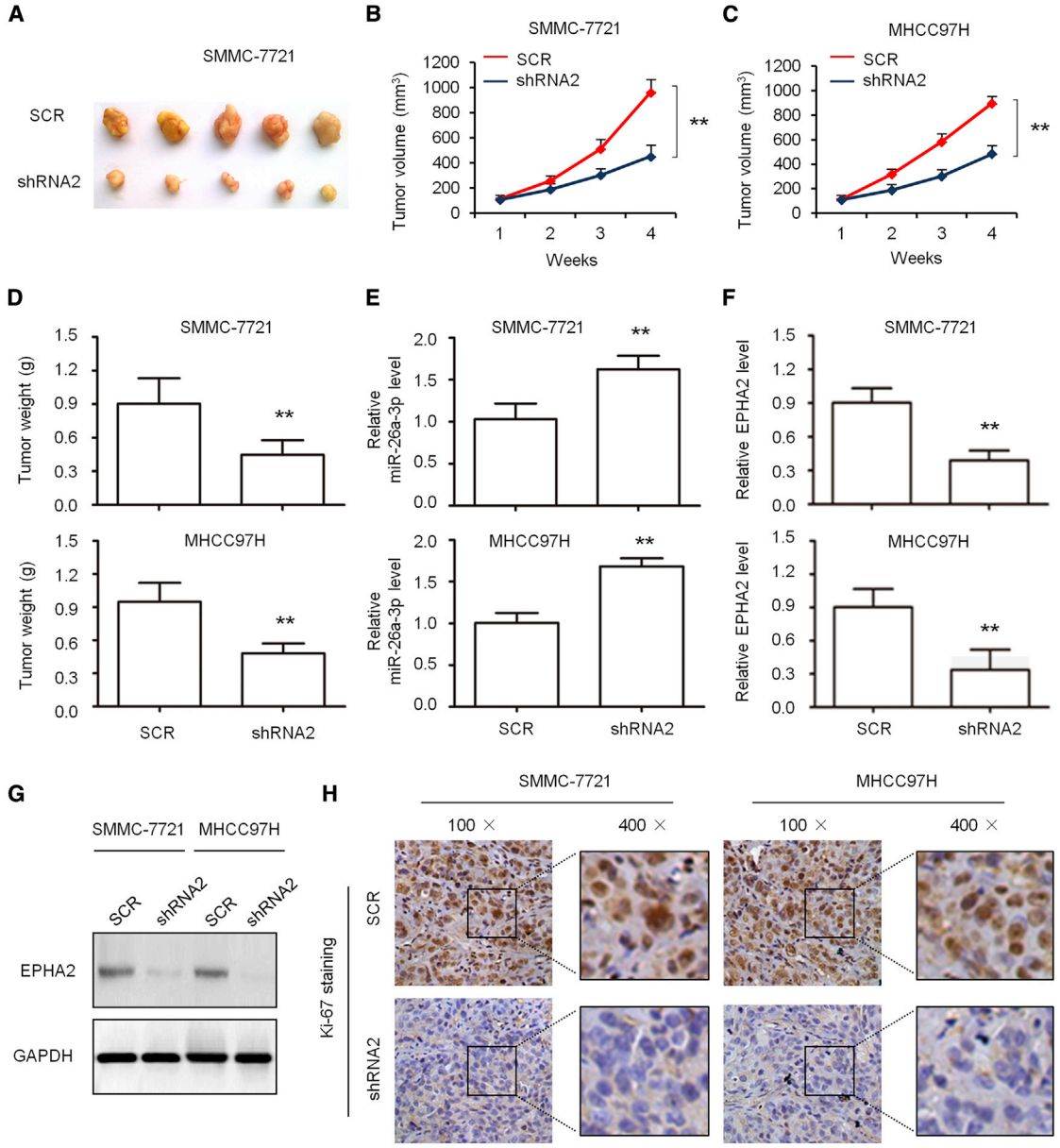

Figure 6. Antitumor Effects of OIP5-AS1 Silencing on Tumor Xenograft Mice

(A) Representative tumor xenograft after the tumors were harvested. (B–D) Growth curve (B, SMMC-7721 cells; C, MHCC97H cells) and tumor weight (D) were measured. (E and F) quantitative real-time PCR detection of the expression levels of hsa-miR-26a-3p (E) and EPHA2 (F) in tumor xenografts. (G) Western blot detection of the protein level of EPHA2 in tumor xenografts. (H) Representative images of immunohistochemical detection of the proliferation index Ki67 *in vivo*. **p < 0.01.

tumor tissues.[50–53] In the process of tumorigenesis and development, lncRNA plays an important role in regulating various biological functions. It has been found that lncRNA HOTAIR and STAT3 co-regulate the migration and invasion of cervical cancer cells.[54] In addition, the expression of lncRNA colorectal cancer-related transcription factor-1 (CCAT1) was increased in gastric cancer, and CCAT1 was closely related to the proliferation and migration of gastric cancer cells.[55] The expression level of lncRNA BANCR in bladder cancer tissue samples was significantly lower than that in paracancerous tissue, and the low expression of BANCR was closely related to the clinical stage of bladder cancer patients.[56]

Since the biological function of lncRNA has been of interest, research on the relationship between the differential expression of lncRNA in tumor and the tumorigenesis mechanism has been gradually carried out and deepened.[57–59] Some lncRNAs have been proven to play an

important role in the occurrence and development of liver cancer, and they are related to the recurrence, metastasis and prognosis of liver cancer. lncRNA HULC is found to be highly express in LIHC, which is related to tumor, node, and metastasis (TNM) stage, intrahepatic metastasis, recurrence, and prognosis.[60] HULC can promote tumor angiogenesis by upregulating the expression of sphingosine kinase 1.[61] The low expression of MEG3 in LIHC can promote the transcriptional activity of p53, change the expression of the p53 target gene, and inhibit the growth of LIHC.[51] Additionally, lncRNA can target transcription factors, RNA polymerases, and so forth to affect gene transcription process and regulate gene transcription and expression.

Many studies have found that the high expression of OIP5-AS1 in lung cancer, breast cancer, multiple myeloma, and other tumors can promote the occurrence and development of tumors.[62–65] Additionally, OIP5-AS1 is a ceRNA in hepatoblastoma cells through modulating miR-186a-5p/ZEB1. Knockdown of OIP5-AS1 expression inhibits proliferation, metastasis, and EMT progress in hepatoblastoma cells through upregulating miR-186a-5p and downregulating ZEB1.[33,66] In this study, our results showed that the expression of OIP5-AS1 in LIHC was significantly higher than that in the matched adjacent tissues, and its high expression was significantly correlated with tumor size and tumor stage. The expression of OIP5-AS1 in the LIHC cell line was significantly higher than that in the normal LIHC cell line. These results suggested that OIP5-AS1 might be involved in the development of LIHC. These data suggest that OIP5-AS1 can be identified as a potential biomarker of prognosis in LIHC patients.

In addition, we found that OIP5-AS1 can promote the proliferation of hepatoma cells, inhibit apoptosis, and enhance cell invasion *in vitro*. In the subcutaneous tumorigenesis experiment of nude mice, OIP5-AS1 was interfered with by shRNA, which significantly inhibited tumor growth and tumor weight; the knockdown of OIP5-AS1 resulted in a significant decrease in the number of proliferation cells stained with Ki67. With regard to the mechanism, our results suggest that lncRNA OIP5-AS1 is a molecular sponge regulating hsa-miR-26a-3p. The inhibition of hsa-miR-26a-3p partially eliminated the effect of OIP5-AS1, resulting in the significant increase of proliferation, invasion, and inhibition of apoptosis in SMMC-7721 and MHCC97H cells inhibited by OIP5-AS1, suggesting that OIP5-AS1 may negatively regulate the proliferation, invasion, and apoptosis of hepatoma cells promoted by hsa-miR-26a-3p.

Furthermore, it was found that EPHA2 was the direct target of hsa-miR-26a-3p. EPHA2 is a kind of Eph receptor tyrosine kinase.[67] It can promote protein tyrosine phosphorylation of its own and downstream substrates by binding to its ligand ephrinal, and then play a role in cell growth and proliferation.[68–70] EPHA2 was found to be highly expressed in breast cancer, gastric cancer, glioblastoma, and other tumors, and it is involved in the growth, differentiation, and proliferation of tumor cells.[71–73] In this study, we found that the expression of EPHA2 was negatively correlated with the expression of hsa-miR-26a-3p, but it was positively correlated with the expression of OIP5-AS1. lncRNA OIP5-AS1 may enhance the function of EPHA2, promote cell proliferation, enhance cell invasion, and inhibit apoptosis by negatively regulating hsa-miR-26a-3p. Therefore, this study deepens our understanding of the pathogenesis of liver cancer and provides an important basis for the prognosis and diagnostic markers of liver cancer.

MATERIALS AND METHODS

Tissue Samples and Cell Lines

A total of 54 paired LIHC tissues and adjacent normal liver tissue samples were collected from patients who received surgery at the Shanghai Tenth People's Hospital, Tongji University School of Medicine between January 2012 and December 2016. None of the patients received adjuvant therapy before surgery. This study protocol was in accordance with the Declaration of Helsinki and approved by the Ethics Committee of the Shanghai Tenth People's Hospital, Tongji University School of Medicine (approval no. SHSY-IEC-2019K10). All of the specimens were immediately frozen in liquid nitrogen and stored at −80°C until use.

The normal liver cell line L02 and five LIHC cell lines (MHCC97H, HepG2, Hep3B, SMMC-7721, and Bel-7402) were purchased from the Institute of Biochemistry and Cell Biology (Shanghai, China). All cells were cultured in DMEM medium (Gibco-BRL, Grand Island, NY, USA) containing 10% fetal bovine serum (FBS), 100 U/mL penicillin, and 100 g/mL streptomycin.

TCGA Data Acquisition and Processing

We downloaded RNA-sequencing data from 371 LIHC patients from TCGA portal (https://www.cancer.gov/about-nci/organization/ccg/research/structural-genomics/tcga), 50 of which had paired normal liver tissues.[74] The lncRNA, microRNA (miRNA), and mRNA expression levels were investigated in 371 LIHC tissues and 50 normal liver tissues in TCGA datasets by Illumina HiSeq 2000 RNA sequencing version 2 analysis and normalized by the RSEM algorithm.[75] The clinical information recorded, including the patient's characteristics, tumor characteristics, and OS, was assessed.

Acquisition of GEO Database Data

The present study downloaded the raw data on GEO: GSE104310, GSE84005, GSE84005, GSE21362, and GSE6857 from the GEO database.[76] The GEO: GSE104310 dataset includes RNA sequence data in 12 tumor samples and 8 non-tumor liver tissues collected from LIHC patients during surgeries at the Sun Yat-sen University Cancer Center, whereas the GEO: GSE84005 dataset includes mRNA expression data from 38 pairs of tumor tissues and adjacent non-tumor tissues from LIHC patients. The GEO: GSE84005 dataset includes gene expression profiles conducted in 68 primary LIHC and 21 noncancerous hepatic tissues. The GEO: GSE21362 dataset includes miRNA expression profiles conducted in 73 paired primary LIHC and noncancerous hepatic tissues. The GEO: GSE6857 dataset includes gene expression profiles conducted in primary LIHC and corresponding noncancerous hepatic tissues from 244 Chinese HCC patients. The present study utilized these sets of differentially expressed

lncRNA, miRNA, and mRNA data to identify differentially expressed genes for LIHC.

RNA Extraction and quantitative real-time PCR

Total RNA from LIHC samples and cell lines was isolated with TRIzol reagent (Life Technologies, Grand Island, NY, USA) according to the manufacturer's protocol.[77] RNA was reverse transcribed into complementary DNA (cDNA) using PrimeScript RT master mix (Takara, Dalian, China), and quantitative real-time PCRwas performed with a SYBR Premix Ex Taq II (perfect real-time) kit (Takara) on an ABI Prism 7900 HT sequence detection system (Applied Biosystems, Foster City, CA, USA).[78] U6 was used as an endogenous control for miRNA, and GAPDH was used for other target genes. The primers used for quantitative real-time PCR were listed as follows: GAPDH, forward, 5′-AGGGCTGCTTTTAACTCTGGT-3′, reverse, 5′-CCCCACTTGATTTTGGAGGGA-3′; EPHA2, forward, 5′-ACCCCCACACATATGAGGAC-3′, reverse, 5′-TGGATGGATCTCGGTAGTGA-3′; and OIP5-AS1, forward, 5′-GGTCGTGAAACACCGTCG-3′, reverse, 5′-GTGGGGCATCCAGGGT-3′. The $2^{-\Delta\Delta CT}$ method was used to analyze expression levels.[79]

Plasmid Construction

The shRNAs targeting OIP5-AS1 were synthesized by Sangon Biotech (Shanghai, China) and inserted into a pLKO.1-TRC cloning vector (Addgene). The target sequence was 5′-GTGACTTAAACAGCTTAAATT-3′ (shRNA1) and 5′-TAAACAGTGACTTTAAATTGT-3′ (shRNA2), respectively. Also, the pLKO.1-TRC control vector was used as a control (named as SCR).

The sequence of the hsa-miR-26a-3p-binding site within the OIP5-AS1 was predicted with starBase 2.0 (http://starbase.sysu.edu.cn). The fragment of OIP5-AS1 and the EPHA2 3′ UTR containing the binding site of hsa-miR-26a-3p were amplified by PCR and cloned into the pmirGLO Dual-Luciferase target expression vector (Promega, Madison, WI, USA).[80] Site mutations were introduced to the WT to construct the MT. All constructions were confirmed by Sanger sequencing.

Cell Transfection and Lentiviral Particles Produced

HEK293T cells were seeded in 96-well plates and cultured for 24 h. Cells were co-transfected with reporter plasmid and hsa-miR-26a-3p mimics or inhibitors. After 24-h transfection, a luciferase assay was determined using the Dual-Luciferase kit (Promega, Madison, WI, USA).

The lentivirus-mediated OIP5-AS1 shRNAs were co-transfected with a packaging system using Lipofectamine 3000 (Thermo Fisher Scientific) in HEK293T cells according to the manufacturer's protocol.[81] LIHC cells were infected with lentiviral particles in the presence of 8 μg/mL Polybrene (Sigma-Aldrich, St. Louis, MO, USA) and selected with 1.5 μg/mL puromycin (Sigma-Aldrich). Suppression of OIP5-AS1 expression was confirmed by quantitative real-time PCR.

Cell Proliferative and Invasion Array

LIHC cells transfected under different conditions were seeded into 96-well plates at a density of 3×10^3 cells per well. Proliferative viability was detected at the indicated time using a Cell Counting Kit-8 (CCK-8, Dojindo, Japan) according to the manufacturer's specifications.[74]

For invasion array, 100 μL of LIHC cells (1×10^5) was suspended in FBS-free medium and seeded into the upper chamber of transwell chamber (Millipore, NY, USA). 600 μL of culture medium containing 20% FBS was added into the lower chamber. After incubation for 24 h at 37°C in 5% CO_2, cells on the upper surface of upper chamber were removed with cotton swabs and stained using 0.5% crystal violet. The number of invaded cell was counted in five random fields under an IX71 microscope (Olympus, Japan).[75]

Chromatin Immunoprecipitation (ChIP)

The ChIP assays were carried out using the Magna ChIP kit (Millipore, Billerica, MA, USA) following the manufacturer's instructions.[76,78,80] First, the crosslink between DNA and proteins was fixated by using formaldehyde for 30 min. Then, the DNAs isolated from LIHC cells were fragmented into 200–1,000 bp using sonication. Subsequently, the fragmented DNAs were incubated overnight with protein A/G beads containing antibodies against EPHA2 or immunoglobulin G (IgG) (negative control). The subsided DNA fragments were determined through quantitative real-time PCR.

Flow Cytometry Analysis

Apoptosis analysis was performed using a fluorescein isothiocyanate (FITC)-annexin V apoptosis detection kit I (BD Biosciences, San Jose, CA, USA).[82] LIHC cells transfected under different conditions were harvested and stained with 5 μL of propidium iodide (PI) and 5 μL of FITC-annexin V. After incubation for 20 min in the dark at room temperature, the stained cells were analyzed using a FACSCalibur flow cytometer (BD Biosciences).[83–85]

Western Blot

Total protein from LIHC cells was extracted using cell lysis buffer. Protein concentration was analyzed using standard procedures for western blotting. After incubation with the appropriate horseradish peroxidase-conjugated secondary antibodies, the membranes were treated with an enhanced chemiluminescence reagent (Merck Millipore, Germany), exposed to X-ray film (Eastman Kodak, Rochester, NY, USA), and quantified by densitometry (Eastman Kodak, Rochester, NY, USA). The rabbit monoclonal antibody for EPHA2 (catalog no. ab185156) and GAPDH antibody (catalog no. ab181602) were purchased from Abcam (Cambridge, MA, USA) and used for western blot analyses. The goat anti-rabbit IgG (Merck) and goat anti-mouse IgG (Merck) antibodies were used for western blot analyses. Antibody dilutions were 1:2,000 for primary antibodies and 1:10,000 for secondary antibodies in western blotting.

Tumor Inoculation Assay in Nude Mice

About 6- to 8-week-old BALB/c male mice were purchased from Shanghai SLAC Laboratory Animal Company (Shanghai, China). All the animals used in this study were approved by the Institutional Animal Care and Use Committee of the Shanghai Tenth People's

Hospital, Tongji University School of Medicine (permit no. 20180426SF). All procedures were performed essentially as previously described.[86] In brief, 1×10^7 viable cells were subcutaneously injected into the flanks of mice. Tumor growth was examined every 3 days using a vernier caliper and the mice were sacrificed 4 weeks later. Subcutaneous xenografts were resected, weighed, and stained for immunohistochemistry (IHC).

Statistical Analysis

All statistical analysis was carried out using GraphPad Prism version 8.0 for Windows (GraphPad, CA, USA). The Student's t test was used for comparison of differences between two groups. Correlations among OIP5-AS1, hsa-miR-26a-3p, and EPHA2 expression were analyzed using a Pearson correlation test. Hierarchical clustering was performed using the multiple experiment viewer (MeV) 4.7.1 software programs. Kaplan-Meier curves and the a log rank test were used to assess the OS of LIHC patients. Data are presented as mean ± standard deviation, and a p value <0.05 was considered statistically significant.

SUPPLEMENTAL INFORMATION

Supplemental Information can be found online at https://doi.org/10.1016/j.omtn.2020.05.032.

AUTHOR CONTRIBUTIONS

Y.-S.M., K.-J.C., C.-C.L., T.-M.W., D.F., and X.-W.Z. designed the study; Y.-S.M., K.-J.C., C.-C.L., T.-M.W., X.-C.Z., J.-B.L., F.Y., Z.-Z.L., J.-H.W., Q.-X.G., B.Y., D.F., and X.-W.Z. conducted the study; Y.-S.M., K.-J.C., C.-C.L., T.-M.W., H.-M.W., L.-P.G., L.L., L.-L.T., Y.S., X.-Q.J., D.F. and X.-W.Z. collected data; Y.-S.M., K.-J.C., C.-C.L., T.-M.W., D.F. and X.-W.Z. performed the statistical analyses and interpreted the data; Y.-S.M., K.-J.C., D.F., and X.-W.Z. contributed to study materials and consumables; Y.-S.M., K.-J.C., C.-C.L., T.-M.W., X.-C.Z., D.F. and X.-W.Z. wrote the manuscript. All authors contributed to the final version of the manuscript and approved the final manuscript.

CONFLICTS OF INTEREST

The authors declare no competing interests.

ACKNOWLEDGMENTS

This study was supported partly by grants from the National Natural Science Foundation of China (81972214, 81972256, 81772932, 81201535, and 81302065); the Nantong Science and Technology Project (JC2018125); the Scientific Research Fund Project of Anhui Medical University (2018xkj058); the Jiangsu 333 Program (BRA2017205); the Nantong Medical Key Talents Training Plan (Key 43); and by the Construction of Clinical Medical Center for Tumor Biological Samples in Nantong (HS2016004).

REFERENCES

1. Wu, S.D., Ma, Y.S., Fang, Y., Liu, L.L., Fu, D., and Shen, X.Z. (2012). Role of the microenvironment in hepatocellular carcinoma development and progression. Cancer Treat. Rev. *38*, 218–225.
2. Liu, L.L., Fu, D., Ma, Y., and Shen, X.Z. (2011). The power and the promise of liver cancer stem cell markers. Stem Cells Dev. *20*, 2023–2030.
3. Shao, M., Yang, Q., Zhu, W., Jin, H., Wang, J., Song, J., Kong, Y., and Lv, X. (2018). lncHOXA10 drives liver TICs self-renewal and tumorigenesis via HOXA10 transcription activation. Mol. Cancer *17*, 173.
4. Kim, Y., Jo, M., Schmidt, J., Luo, X., Prakash, T.P., Zhou, T., Klein, S., Xiao, X., Post, N., Yin, Z., and MacLeod, A.R. (2019). Enhanced potency of GalNAc-conjugated antisense oligonucleotides in hepatocellular cancer models. Mol. Ther. *27*, 1547–1557.
5. Suksanpaisan, L., Xu, R., Tesfay, M.Z., Bomidi, C., Hamm, S., Vandergaast, R., Jenks, N., Steele, M.B., Ota-Setlik, A., Akhtar, H., et al. (2018). Preclinical development of oncolytic immunovirotherapy for treatment of HPV^{POS} cancers. Mol. Ther. Oncolytics *10*, 1–13.
6. Wang, H., Chen, W., Jin, M., Hou, L., Chen, X., Zhang, R., Zhang, J., and Zhu, J. (2018). circSLC3A2 functions as an oncogenic factor in hepatocellular carcinoma by sponging miR-490-3p and regulating PPM1F expression. Mol. Cancer *17*, 165.
7. Yang, Y.F., Zhang, M.F., Tian, Q.H., Fu, J., Yang, X., Zhang, C.Z., and Yang, H. (2018). SPAG5 interacts with CEP55 and exerts oncogenic activities via PI3K/AKT pathway in hepatocellular carcinoma. Mol. Cancer *17*, 117.
8. Fu, D., Ma, Y., Wu, W., Zhu, X., Jia, C., Zhao, Q., Zhang, C., and Wu, X.Z. (2009). Cell-cycle-dependent PC-PLC regulation by APC/C^{Cdc20}-mediated ubiquitin-proteasome pathway. J. Cell. Biochem. *107*, 686–696.
9. Yu, M., Luo, H., Fan, M., Wu, X., Shi, B., Di, S., Liu, Y., Pan, Z., Jiang, H., and Li, Z. (2018). Development of GPC3-specific chimeric antigen receptor-engineered natural killer cells for the treatment of hepatocellular carcinoma. Mol. Ther. *26*, 366–378.
10. Peng, E.Y., Shu, Y., Wu, Y., Zeng, F., Tan, S., Deng, Y., Deng, Y., Chen, H., Zhu, L., and Xu, H. (2018). Presence and diagnostic value of circulating tsncRNA for ovarian tumor. Mol. Cancer *17*, 163.
11. Ma, M., Zhang, Y., Weng, M., Hu, Y., Xuan, Y., Hu, Y., and Lv, K. (2018). lncRNA GCAWKR promotes gastric cancer development by scaffolding the chromatin modification factors WDR5 and KAT2A. Mol. Ther. *26*, 2658–2668.
12. Horita, K., Kurosaki, H., Nakatake, M., Kuwano, N., Oishi, T., Itamochi, H., Sato, S., Kono, H., Ito, M., Hasegawa, K., et al. (2019). lncRNA UCA1-mediated Cdc42 signaling promotes oncolytic vaccinia virus cell-to-cell spread in ovarian cancer. Mol. Ther. Oncolytics *13*, 35–48.
13. Huang, Y., Xiang, B., Liu, Y., Wang, Y., and Kan, H. (2018). lncRNA CDKN2B-AS1 promotes tumor growth and metastasis of human hepatocellular carcinoma by targeting let-7c-5p/NAP1L1 axis. Cancer Lett. *437*, 56–66.
14. Liu, H., Deng, H., Zhao, Y., Li, C., and Liang, Y. (2018). lncRNA XIST/miR-34a axis modulates the cell proliferation and tumor growth of thyroid cancer through MET-PI3K-AKT signaling. J. Exp. Clin. Cancer Res. *37*, 279.
15. Li, Q., Dong, C., Cui, J., Wang, Y., and Hong, X. (2018). Over-expressed lncRNA HOTAIRM1 promotes tumor growth and invasion through up-regulating HOXA1 and sequestering G9a/EZH2/Dnmts away from the *HOXA1* gene in glioblastoma multiforme. J. Exp. Clin. Cancer Res. *37*, 265.
16. Wang, R., Ma, Z., Feng, L., Yang, Y., Tan, C., Shi, Q., Lian, M., He, S., Ma, H., and Fang, J. (2018). lncRNA MIR31HG targets HIF1A and P21 to facilitate head and neck cancer cell proliferation and tumorigenesis by promoting cell-cycle progression. Mol. Cancer *17*, 162.
17. Santos, J.M., Cervera-Carrascon, V., Havunen, R., Zafar, S., Siurala, M., Sorsa, S., Anttila, M., Kanerva, A., and Hemminki, A. (2018). Adenovirus coding for interleukin-2 and tumor necrosis factor alpha replaces lymphodepleting chemotherapy in adoptive T cell therapy. Mol. Ther. *26*, 2243–2254.
18. Zeng, C., Liu, S., Lu, S., Yu, X., Lai, J., Wu, Y., Chen, S., Wang, L., Yu, Z., Luo, G., and Li, Y. (2018). The c-Myc-regulated lncRNA NEAT1 and paraspeckles modulate imatinib-induced apoptosis in CML cells. Mol. Cancer *17*, 130.
19. Xie, S., Yu, X., Li, Y., Ma, H., Fan, S., Chen, W., Pan, G., Wang, W., Zhang, H., Li, J., and Lin, Z. (2018). Upregulation of lncRNA ADAMTS9-AS2 promotes salivary adenoid cystic carcinoma metastasis via PI3K/Akt and MEK/Erk signaling. Mol. Ther. *26*, 2766–2778.
20. Wang, Y., Zhang, X., Wang, Z., Hu, Q., Wu, J., Li, Y., Ren, X., Wu, T., Tao, X., Chen, X., et al. (2018). lncRNA-p23154 promotes the invasion-metastasis potential of oral

squamous cell carcinoma by regulating Glut1-mediated glycolysis. Cancer Lett. *434*, 172–183.

21. Yu, J., Han, Z., Sun, Z., Wang, Y., Zheng, M., and Song, C. (2018). lncRNA SLCO4A1-AS1 facilitates growth and metastasis of colorectal cancer through β-catenin-dependent Wnt pathway. J. Exp. Clin. Cancer Res. *37*, 222.

22. Gu, J., Wang, Y., Wang, X., Zhou, D., Shao, C., Zhou, M., and He, Z. (2018). Downregulation of lncRNA GAS5 confers tamoxifen resistance by activating miR-222 in breast cancer. Cancer Lett. *434*, 1–10.

23. Sun, L.Y., Li, X.J., Sun, Y.M., Huang, W., Fang, K., Han, C., Chen, Z.H., Luo, X.Q., Chen, Y.Q., and Wang, W.T. (2018). lncRNA ANRIL regulates AML development through modulating the glucose metabolism pathway of AdipoR1/AMPK/SIRT1. Mol. Cancer *17*, 127.

24. Xu, H., Chen, G.F., Ma, Y.S., Zhang, H.W., Zhou, Y., Liu, G.H., Chen, D.Y., Ping, J., Liu, Y.H., Mou, X., and Fu, D. (2020). Hepatic proteomic changes and Sirt1/AMPK signaling activation by oxymatrine treatment in rats with non-alcoholic steatosis. Front. Pharmacol. *11*, 216.

25. Yoshida, S., Miyagawa, S., Fukushima, S., Kawamura, T., Kashiyama, N., Ohashi, F., Toyofuku, T., Toda, K., and Sawa, Y. (2018). Maturation of human induced pluripotent stem cell-derived cardiomyocytes by soluble factors from human mesenchymal stem cells. Mol. Ther. *26*, 2681–2695.

26. Hemminki, O., Oksanen, M., Taipale, K., Liikanen, I., Koski, A., Joensuu, T., Kanerva, A., and Hemminki, A. (2018). Oncograms visualize factors influencing long-term survival of cancer patients treated with adenoviral oncolytic immunotherapy. Mol. Ther. Oncolytics *9*, 41–50.

27. Ma, Y.S., Wang, X.F., Yu, F., Wu, T.M., Liu, J.B., Zhang, Y.J., Xia, Q., Jiang, Z.Y., Lin, Q.L., and Fu, D. (2020). Inhibition of USP14 and UCH37 deubiquitinating activity by b-AP15 as a potential therapy for tumors with p53 deficiency. Sig. Transduct. Target. Ther. 5, 30, https://doi.org/10.1038/s41392-020-0143-9.

28. Ma, Y.S., Wang, X.F., Zhang, Y.J., Luo, P., Long, H.D., Li, L., Yang, H.Q., Xie, R.T., Jia, C.Y., Lu, G.X., et al. (2020). Inhibition of USP14 deubiquitinating activity as a potential therapy for tumors with *p53* deficiency. Mol. Ther. Oncolytics *16*, 147–157.

29. Fahrer, J. (2020). Switching off DNA repair-how colorectal cancer evades targeted therapies through adaptive mutability. Sig. Transduct. Target. Ther. 5, 19, https://doi.org/10.1038/s41392-020-0120-3.

30. Ballesteros-Briones, M.C., Martisova, E., Casales, E., Silva-Pilipich, N., Buñuales, M., Galindo, J., Mancheño, U., Gorraiz, M., Lasarte, J.J., Kochan, G., et al. (2019). Short-term local expression of a PD-L1 blocking antibody from a self-replicating RNA vector induces potent antitumor responses. Mol. Ther. *27*, 1892–1905.

31. Kim, Y.J., Baek, D.S., Lee, S., Park, D., Kang, H.N., Cho, B.C., and Kim, Y.S. (2019). Dual-targeting of EGFR and Neuropilin-1 attenuates resistance to EGFR-targeted antibody therapy in KRAS-mutant non-small cell lung cancer. Cancer Lett. *466*, 23–34.

32. Ma, Y.S., Wu, Z.J., Zhang, H.W., Cai, B., Huang, T., Long, H.D., Xu, H., Zhao, Y.Z., Yin, Y.Z., Xue, S.B., et al. (2019). Dual regulatory mechanisms of expression and mutation involving metabolism-related genes FDFT1 and UQCR5 during CLM. Mol. Ther. Oncolytics *14*, 172–178.

33. Fergusson, D.A., Wesch, N.L., Leung, G.J., MacNeil, J.L., Conic, I., Presseau, J., Cobey, K.D., Diallo, J.S., Auer, R., Kimmelman, J., et al. (2019). Assessing the completeness of reporting in preclinical oncolytic virus therapy studies. Mol. Ther. Oncolytics *14*, 179–187.

34. Rodrigues, D., Souza, T., Jennen, D.G.J., Lemmens, L., Kleinjans, J.C.S., and de Kok, T.M. (2019). Drug-induced gene expression profile changes in relation to intestinal toxicity: state-of-the-art and new approaches. Cancer Treat. Rev. *77*, 57–66.

35. Leslie, T.K., James, A.D., Zaccagna, F., Grist, J.T., Deen, S., Kennerley, A., Riemer, F., Kaggie, J.D., Gallagher, F.A., Gilbert, F.J., and Brackenbury, W.J. (2019). Sodium homeostasis in the tumour microenvironment. Biochim. Biophys. Acta Rev. Cancer *1872*, 188304.

36. Jimenez Calvente, C., Del Pilar, H., Tameda, M., Johnson, C.D., and Feldstein, A.E. (2020). MicroRNA 223 3p negatively regulates the NLRP3 inflammasome in acute and chronic liver injury. Mol. Ther. *28*, 653–663.

37. Liu, W.T., Wang, Y., Zhang, J., Ye, F., Huang, X.H., Li, B., and He, Q.Y. (2018). A novel strategy of integrated microarray analysis identifies CENPA, CDK1 and CDC20 as a cluster of diagnostic biomarkers in lung adenocarcinoma. Cancer Lett. *425*, 43–53.

38. Ma, Y.S., Lv, Z.W., Yu, F., Chang, Z.Y., Cong, X.L., Zhong, X.M., Lu, G.X., Zhu, J., and Fu, D. (2018). MicroRNA-302a/d inhibits the self-renewal capability and cell cycle entry of liver cancer stem cells by targeting the E2F7/AKT axis. J. Exp. Clin. Cancer Res. *37*, 252.

39. Ma, Y.S., Yu, F., Zhong, X.M., Lu, G.X., Cong, X.L., Xue, S.B., Xie, W.T., Hou, L.K., Pang, L.J., Wu, W., et al. (2018). miR-30 family reduction maintains self-renewal and promotes tumorigenesis in NSCLC-initiating cells by targeting oncogene TM4SF1. Mol. Ther. *26*, 2751–2765.

40. Lv, D., Ma, Q.H., Duan, J.J., Wu, H.B., Zhao, X.L., Yu, S.C., and Bian, X.W. (2016). Optimized dissociation protocol for isolating human glioma stem cells from tumorspheres via fluorescence-activated cell sorting. Cancer Lett. *377*, 105–115.

41. Jia, H., Qi, H., Gong, Z., Yang, S., Ren, J., Liu, Y., Li, M.Y., and Chen, G.G. (2019). The expression of FOXP3 and its role in human cancers. Biochim. Biophys. Acta Rev. Cancer *1871*, 170–178.

42. Xin, X., Wu, M., Meng, Q., Wang, C., Lu, Y., Yang, Y., Li, X., Zheng, Q., Pu, H., Gui, X., et al. (2018). Long noncoding RNA HULC accelerates liver cancer by inhibiting PTEN via autophagy cooperation to miR15a. Mol. Cancer *17*, 94.

43. Liu, B., Jiang, S., Li, M., Xiong, X., Zhu, M., Li, D., Zhao, L., Qian, L., Zhai, L., Li, J., et al. (2018). Proteome-wide analysis of USP14 substrates revealed its role in hepatosteatosis via stabilization of FASN. Nat. Commun. *9*, 4770.

44. Wu, X., Luo, H., Shi, B., Di, S., Sun, R., Su, J., Liu, Y., Li, H., Jiang, H., and Li, Z. (2019). Combined antitumor effects of sorafenib and GPC3-CAR T cells in mouse models of hepatocellular carcinoma. Mol. Ther. *27*, 1483–1494.

45. Fan, H., Lv, P., Mu, T., Zhao, X., Liu, Y., Feng, Y., Lv, J., Liu, M., and Tang, H. (2018). lncRNA n335586/miR-924/CKMT1A axis contributes to cell migration and invasion in hepatocellular carcinoma cells. Cancer Lett. *429*, 89–99.

46. Zhou, W., Gong, L., Wu, Q., Xing, C., Wei, B., Chen, T., Zhou, Y., Yin, S., Jiang, B., Xie, H., et al. (2018). PHF8 upregulation contributes to autophagic degradation of E-cadherin, epithelial-mesenchymal transition and metastasis in hepatocellular carcinoma. J. Exp. Clin. Cancer Res. *37*, 215.

47. Dong, H., Wang, W., Mo, S., Chen, R., Zou, K., Han, J., Zhang, F., and Hu, J. (2018). SP1-induced lncRNA AGAP2-AS1 expression promotes chemoresistance of breast cancer by epigenetic regulation of MyD88. J. Exp. Clin. Cancer Res. *37*, 202.

48. Yuan, H., Chen, Z., Bai, S., Wei, H., Wang, Y., Ji, R., Guo, Q., Li, Q., Ye, Y., Wu, J., et al. (2018). Molecular mechanisms of lncRNA SMARCC2/miR-551b-3p/TMPRSS4 axis in gastric cancer. Cancer Lett. *418*, 84–96.

49. Li, X.N., Wang, Z.J., Ye, C.X., Zhao, B.C., Li, Z.L., and Yang, Y. (2018). RNA sequencing reveals the expression profiles of circRNA and indicates that circDDX17 acts as a tumor suppressor in colorectal cancer. J. Exp. Clin. Cancer Res. *37*, 325.

50. Zhang, G., Li, S., Lu, J., Ge, Y., Wang, Q., Ma, G., Zhao, Q., Wu, D., Gong, W., Du, M., et al. (2018). lncRNA *MT1JP* functions as a ceRNA in regulating FBXW7 through competitively binding to miR-92a-3p in gastric cancer. Mol. Cancer *17*, 87.

51. Huang, K.W., Reebye, V., Czysz, K., Ciriello, S., Dorman, S., Reccia, I., Lai, H.S., Peng, L., Kostomitsopoulos, N., Nicholls, J., et al. (2020). Liver activation of hepatocellular nuclear factor-4α by small activating rna rescues dyslipidemia and improves metabolic profile. Mol. Ther. Nucleic Acids *19*, 361–370.

52. Ma, Y., Zhang, J., Wen, L., and Lin, A. (2018). Membrane-lipid associated lncRNA: a new regulator in cancer signaling. Cancer Lett. *419*, 27–29.

53. Kang, M., Ren, M., Li, Y., Fu, Y., Deng, M., and Li, C. (2018). Exosome-mediated transfer of lncRNA PART1 induces gefitinib resistance in esophageal squamous cell carcinoma via functioning as a competing endogenous RNA. J. Exp. Clin. Cancer Res. *37*, 171.

54. Rogers, G.L., Chen, H.Y., Morales, H., and Cannon, P.M. (2019). Homologous recombination-based genome editing by clade F AAVs is inefficient in the absence of a targeted DNA break. Mol. Ther. *27*, 1726–1736.

55. Matés, J.M., Campos-Sandoval, J.A., Santos-Jiménez, J.L., and Márquez, J. (2019). Dysregulation of glutaminase and glutamine synthetase in cancer. Cancer Lett. *467*, 29–39.

56. He, A., Liu, Y., Chen, Z., Li, J., Chen, M., Liu, L., Liao, X., Lv, Z., Zhan, Y., Zhuang, C., et al. (2016). Over-expression of long noncoding RNA BANCR inhibits malignant phenotypes of human bladder cancer. J. Exp. Clin. Cancer Res. *35*, 125.

57. Tang, Y., He, Y., Zhang, P., Wang, J., Fan, C., Yang, L., Xiong, F., Zhang, S., Gong, Z., Nie, S., et al. (2018). lncRNAs regulate the cytoskeleton and related Rho/ROCK signaling in cancer metastasis. Mol. Cancer *17*, 77.

58. Zhao, X., Sun, J., Chen, Y., Su, W., Shan, H., Li, Y., Wang, Y., Zheng, N., Shan, H., and Liang, H. (2018). lncRNA PFAR promotes lung fibroblast activation and fibrosis by targeting miR-138 to regulate the YAP1-twist axis. Mol. Ther. *26*, 2206–2217.

59. Yue, B., Liu, C., Sun, H., Liu, M., Song, C., Cui, R., Qiu, S., and Zhong, M. (2018). A positive feed-forward loop between lncRNA-CYTOR and Wnt/β-catenin signaling promotes metastasis of colon cancer. Mol. Ther. *26*, 1287–1298.

60. Boesch, M., Baty, F., Rumpold, H., Sopper, S., Wolf, D., and Brutsche, M.H. (2019). Fibroblasts in cancer: defining target structures for therapeutic intervention. Biochim. Biophys. Acta Rev. Cancer *1872*, 111–121.

61. Liu, Y., Feng, J., Sun, M., Yang, G., Yuan, H., Wang, Y., Bu, Y., Zhao, M., Zhang, S., and Zhang, X. (2019). Long non-coding RNA HULC activates HBV by modulating HBx/STAT3/miR-539/APOBEC3B signaling in HBV-related hepatocellular carcinoma. Cancer Lett. *454*, 158–170.

62. Tomasetti, C., Poling, J., Roberts, N.J., London, N.R., Jr., Pittman, M.E., Haffner, M.C., Rizzo, A., Baras, A., Karim, B., Kim, A., et al. (2019). Cell division rates decrease with age, providing a potential explanation for the age-dependent deceleration in cancer incidence. Proc. Natl. Acad. Sci. USA *116*, 20482–20488.

63. Alečković, M., McAllister, S.S., and Polyak, K. (2019). Metastasis as a systemic disease: molecular insights and clinical implications. Biochim. Biophys. Acta Rev. Cancer *1872*, 89–102.

64. Rimassa, L., Danesi, R., Pressiani, T., and Merle, P. (2019). Management of adverse events associated with tyrosine kinase inhibitors: Improving outcomes for patients with hepatocellular carcinoma. Cancer Treat. Rev. *77*, 20–28.

65. Ho, D.W., Tsui, Y.M., Sze, K.M., Chan, L.K., Cheung, T.T., Lee, E., Sham, P.C., Tsui, S.K., Lee, T.K., and Ng, I.O. (2019). Single-cell transcriptomics reveals the landscape of intra-tumoral heterogeneity and stemness-related subpopulations in liver cancer. Cancer Lett. *459*, 176–185.

66. Li, Y., Han, X., Feng, H., and Han, J. (2019). Long noncoding RNA OIP5-AS1 in cancer. Clin. Chim. Acta *499*, 75–80.

67. Conejo-Garcia, J.R. (2019). Breaking barriers for T cells by targeting the EPHA2/TGF-β/COX-2 axis in pancreatic cancer. J. Clin. Invest. *130*, 3521–3523.

68. Tahmasebi-Birgani, M., Ansari, H., and Carloni, V. (2019). Defective mitosis-linked DNA damage response and chromosomal instability in liver cancer. Biochim. Biophys. Acta Rev. Cancer *1872*, 60–65.

69. Chen, Z., Liu, Z., Zhang, M., Huang, W., Li, Z., Wang, S., Zhang, C., Dong, B., Gao, J., and Shen, L. (2019). EPHA2 blockade reverses acquired resistance to afatinib induced by EPHA2-mediated MAPK pathway activation in gastric cancer cells and avatar mice. Int. J. Cancer *145*, 2440–2449.

70. Lévêque, R., Corbet, C., Aubert, L., Guilbert, M., Lagadec, C., Adriaenssens, E., Duval, J., Finetti, P., Birnbaum, D., Magné, N., et al. (2019). ProNGF increases breast tumor aggressiveness through functional association of TrkA with EphA2. Cancer Lett. *449*, 196–206.

71. Li, J.Y., Xiao, T., Yi, H.M., Yi, H., Feng, J., Zhu, J.F., Huang, W., Lu, S.S., Zhou, Y.H., Li, X.H., and Xiao, Z.Q. (2019). S897 phosphorylation of EphA2 is indispensable for EphA2-dependent nasopharyngeal carcinoma cell invasion, metastasis and stem properties. Cancer Lett. *444*, 162–174.

72. De Robertis, M., Mazza, T., Fusilli, C., Loiacono, L., Poeta, M.L., Sanchez, M., Massi, E., Lamorte, G., Diodoro, M.G., Pescarmona, E., et al. (2018). EphB2 stem-related and EphA2 progression-related miRNA-based networks in progressive stages of CRC evolution: clinical significance and potential miRNA drivers. Mol. Cancer *17*, 169.

73. Nikas, I., Ryu, H.S., and Theocharis, S. (2018). Viewing the Eph receptors with a focus on breast cancer heterogeneity. Cancer Lett. *434*, 160–171.

74. Livak, K.J., and Schmittgen, T.D. (2001). Analysis of relative gene expression data using real-time quantitative PCR and the $2^{-\Delta\Delta C(T)}$ method. Methods *25*, 402–408.

75. Dong, P., Xiong, Y., Yue, J., Xu, D., Ihira, K., Konno, Y., Kobayashi, N., Todo, Y., and Watari, H. (2019). Long noncoding RNA NEAT1 drives aggressive endometrial cancer progression via miR-361-regulated networks involving STAT3 and tumor microenvironment-related genes. J. Exp. Clin. Cancer Res. *38*, 295.

76. Ma, Y.S., Wu, Z.J., Bai, R.Z., Dong, H., Xie, B.X., Wu, X.H., Hang, X.S., Liu, A.N., Jiang, X.H., Wang, G.R., et al. (2018). DRR1 promotes glioblastoma cell invasion and epithelial-mesenchymal transition via regulating AKT activation. Cancer Lett. *423*, 86–94.

77. Wang, H.L., Liu, P.F., Yue, J., Jiang, W.H., Cui, Y.L., Ren, H., Wang, H., Zhuang, Y., Liu, Y., Jiang, D., et al. (2020). Somatic gene mutation signatures predict cancer type and prognosis in multiple cancers with pan-cancer 1000 gene panel. Cancer Lett. *470*, 181–190.

78. Chen, Y., Zhao, H., Li, H., Feng, X., Tang, H., Qiu, C., Zhang, J., and Fu, B. (2020). LINC01234/microRNA-31-5p/MAGEA3 axis mediates the proliferation and chemoresistance of hepatocellular carcinoma cells. Mol. Ther. Nucleic Acids *19*, 168–178.

79. Xiao, Y., Najeeb, R.M., Ma, D., Yang, K., Zhong, Q., and Liu, Q. (2019). Upregulation of CENPM promotes hepatocarcinogenesis through mutiple mechanisms. J. Exp. Clin. Cancer Res. *38*, 458.

80. Zhang, Y., Song, J., Zhao, Z., Yang, M., Chen, M., Liu, C., Ji, J., and Zhu, D. (2020). Single-cell transcriptome analysis reveals tumor immune microenvironment heterogenicity and granulocytes enrichment in colorectal cancer liver metastases. Cancer Lett. *470*, 84–94.

81. Xiao, Y., Najeeb, R.M., Ma, D., Yang, K., Zhong, Q., and Liu, Q. (2019). Upregulation of CENPM promotes hepatocarcinogenesis through mutiple mechanisms. J. Exp. Clin. Cancer Res. *38*, 458.

82. Chen, Y., Peng, C., Chen, J., Chen, D., Yang, B., He, B., Hu, W., Zhang, Y., Liu, H., Dai, L., et al. (2019). WTAP facilitates progression of hepatocellular carcinoma via m6A-HuR-dependent epigenetic silencing of ETS1. Mol. Cancer *18*, 127.

83. Unfried, J.P., Serrano, G., Suárez, B., Sangro, P., Ferretti, V., Prior, C., Boix, L., Bruix, J., Sangro, B., Segura, V., and Fortes, P. (2019). Identification of coding and long noncoding RNAs differentially expressed in tumors and preferentially expressed in healthy tissues. Cancer Res. *79*, 5167–5180.

84. Vivekanadhan, S., and Mukhopadhyay, D. (2019). Divergent roles of Plexin D1 in cancer. Biochim. Biophys. Acta Rev. Cancer *1872*, 103–110.

85. Tam, B.Y., Chiu, K., Chung, H., Bossard, C., Nguyen, J.D., Creger, E., Eastman, B.W., Mak, C.C., Ibanez, M., Ghias, A., et al. (2020). The CLK inhibitor SM08502 induces anti-tumor activity and reduces Wnt pathway gene expression in gastrointestinal cancer models. Cancer Lett. *473*, 186–197.

86. Cultrara, C.N., Shah, S., Antuono, G., Heller, C.J., Ramos, J.A., Samuni, U., Zilberberg, J., and Sabatino, D. (2019). Size matters: arginine-derived peptides targeting the PSMA receptor can efficiently complex but not transfect siRNA. Mol. Ther. Nucleic Acids *18*, 863–870.

OMTN, Volume *21*

Supplemental Information

Long Noncoding RNA OIP5-AS1 Promotes the Progression of Liver Hepatocellular Carcinoma via Regulating the hsa-miR-26a-3p/EPHA2 Axis

Yu-Shui Ma, Kai-Jian Chu, Chang-Chun Ling, Ting-Miao Wu, Xu-Chao Zhu, Ji-Bin Liu, Fei Yu, Zhi-Zhen Li, Jing-Han Wang, Qing-Xiang Gao, Bin Yi, Hui-Min Wang, Li-Peng Gu, Liu Li, Lin-Lin Tian, Yi Shi, Xiao-Qing Jiang, Da Fu, and Xiong-Wen Zhang

Supplemental Information

Long noncoding RNA OIP5-AS1 promotes the progression of liver hepatocellular carcinoma via regulating hsa-miR-26a-3p/EPHA2 axis

Supplemental information contains three supplemental figures and legends.

Supplementary figure and legend

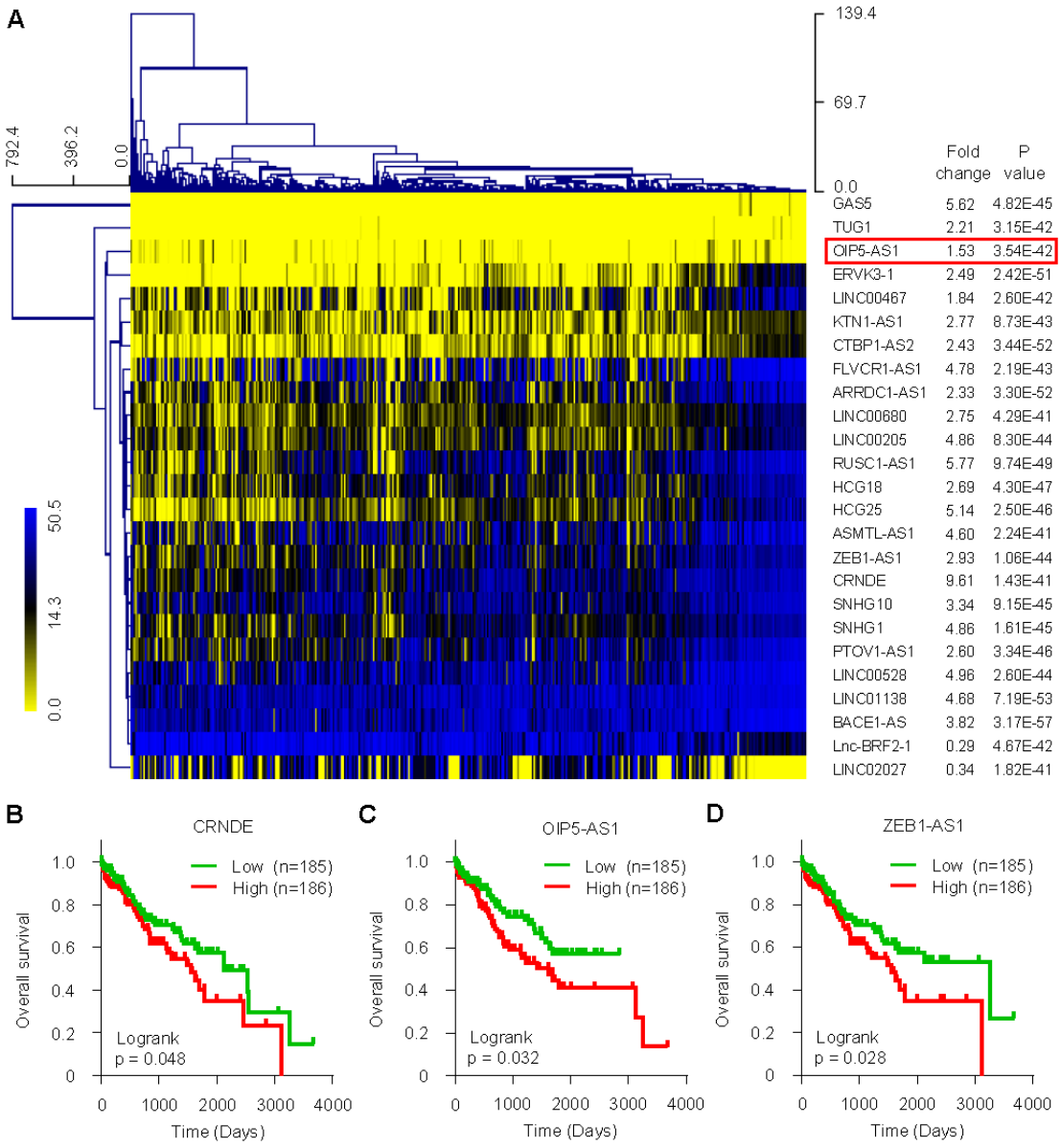

Supplementary Figure 1. Identification of significantly dysregulated lncRNAs in LIHC. (A) Hierarchical clustering of significantly dysregulated lncRNAs in LIHC was performed using the multiple experiment viewer 4.7.1 software programs. (B-D) The Kaplan-Meier method was used to evaluate the relationship between lncRNA CRNDE (B), OIP5-AS1 (C) and ZEB1-AS1 (D) expression and overall survival of 371 LIHC patients from TCGA datasets.

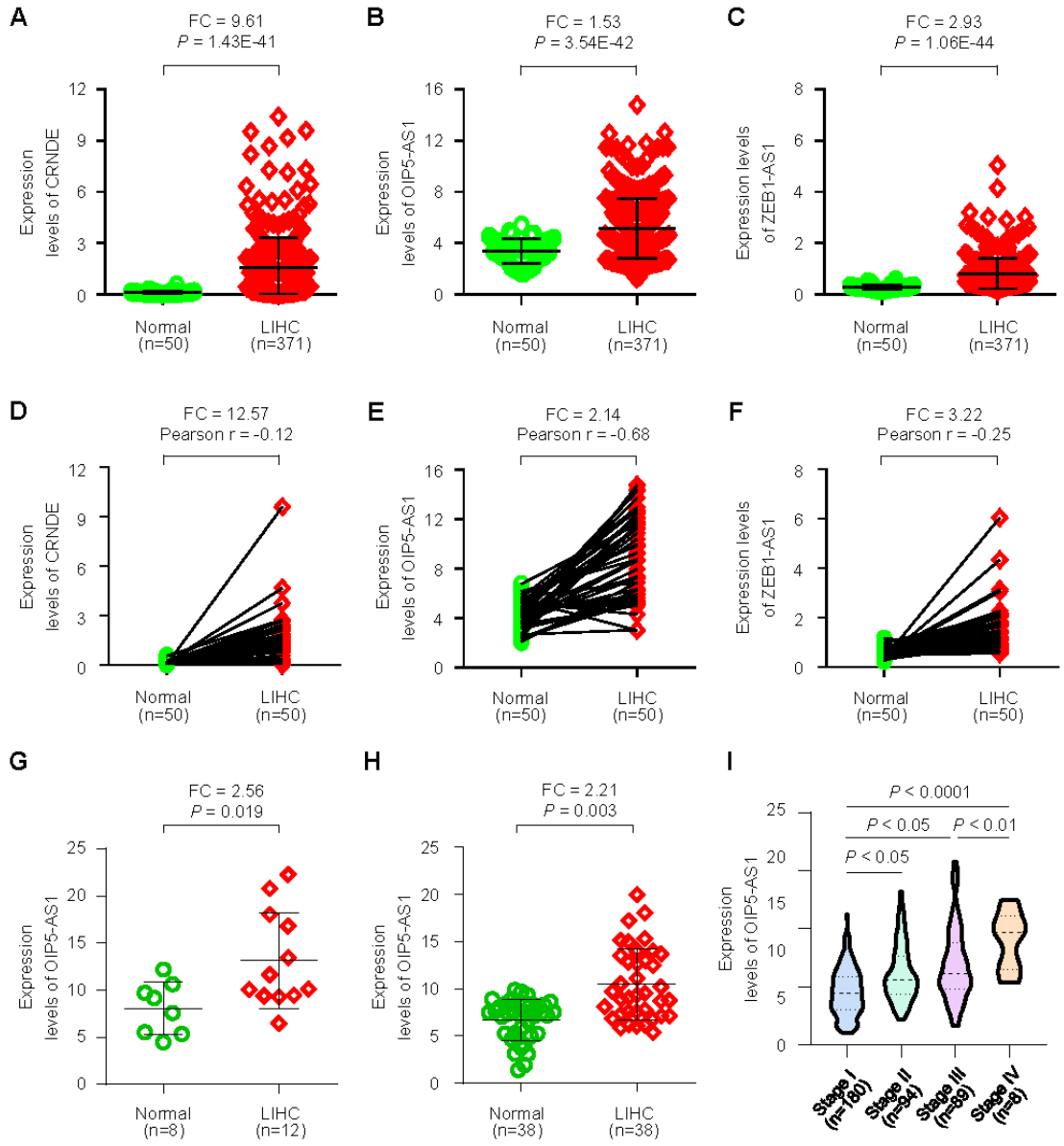

Supplementary Figure 2. The expression of OIP5-AS1 in LIHC samples. (A-C) The expression level of CRNDE (A), OIP5-AS1 (B) and ZEB1-AS1 (C) in 371 LIHC tissues and 50 adjacent noncancerous tissues. (D-F) The correlation of CRNDE (D), OIP5-AS1 (E) and ZEB1-AS1 (F) in 371 LIHC tissues and 50 adjacent noncancerous tissues. (G) OIP5-AS1 expression level was examined in GSE104310 dataset. (H) OIP5-AS1 expression level was examined in GSE84005 dataset. (I) The correlation of OIP5-AS1 expression level and tumor stage in 371 LIHC patients.

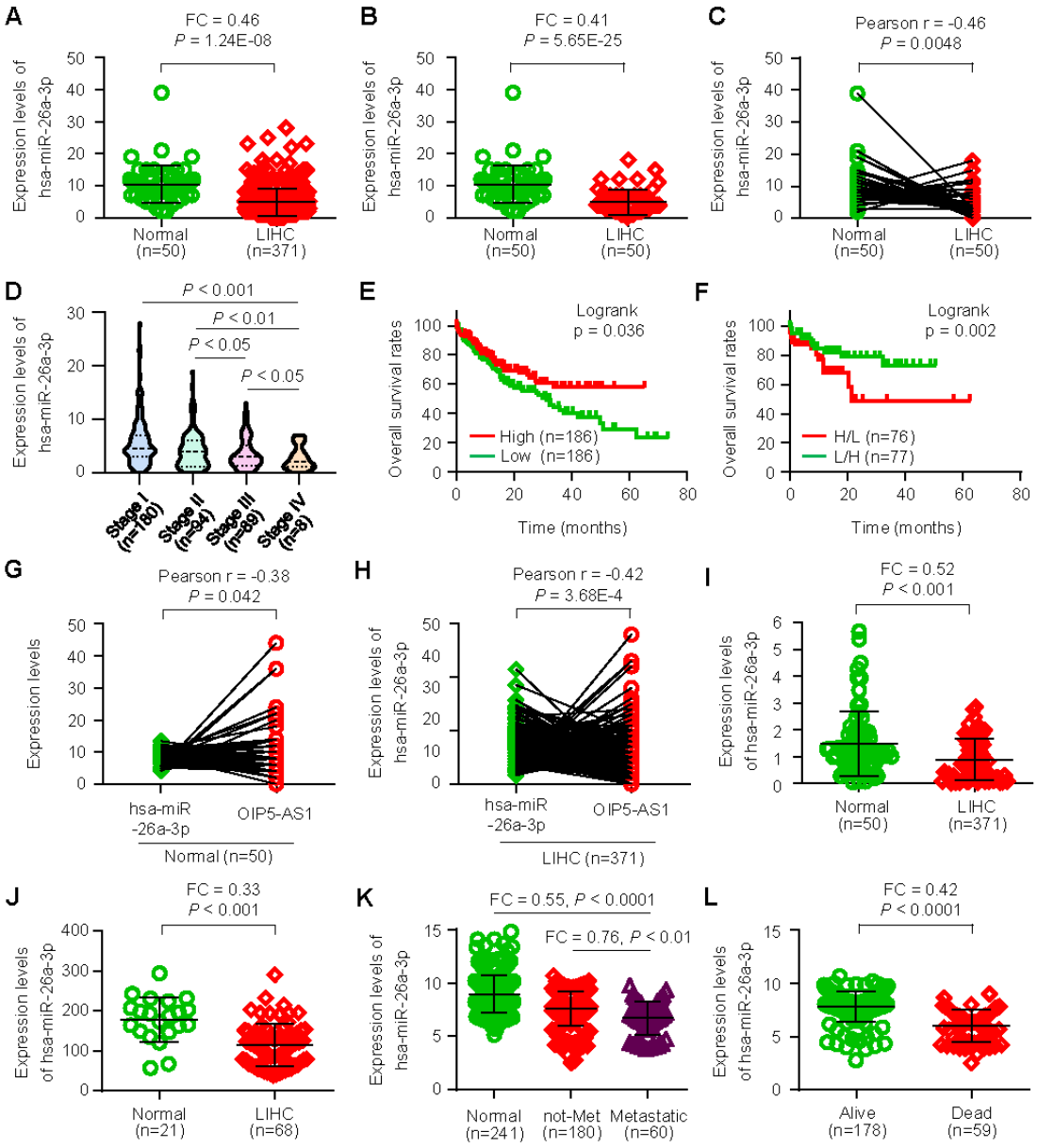

Supplementary Figure 3. The expression and prognostic value of hsa-miR-26a-3p and in LIHC samples. (A) The expression level of hsa-miR-26a-3p in 371 LIHC tissues and 50 adjacent noncancerous tissues. (B, C) The expression level (B) and correlation (C) of hsa-miR-26a-3p in 50 pairs of LIHC tissues and adjacent noncancerous tissues. (D) The correlation of hsa-miR-26a-3p expression level and tumor stage in 371 LIHC patients. (E) The Kaplan-Meier method was used to evaluate the relationship between hsa-miR-26a-3p expression and overall survival of 371 LIHC patients. (F) The Kaplan-Meier method was used to evaluate the relationship between OIP5-AS1/hsa-miR-26a-3p expression and overall survival of 371 LIHC

patients. H/L, high OIP5-AS1 and low hsa-miR-26a-3p expression; L/H, low OIP5-AS1 and high hsa-miR-26a-3p expression. (G, H) The correlation between hsa-miR-26a-3p and OIP5-AS1 in 50 adjacent noncancerous tissues (H) and 371 LIHC tissues (G). (I) Hsa-miR-26a-3p expression level was examined in GSE21362 dataset. (J) Hsa-miR-26a-3p expression level was examined in GSE36915 dataset. (K) Hsa-miR-26a-3p expression level in 241 adjacent noncancerous tissues, 180 non-metastatic and 60 metastatic LIHC tissues from GSE6857 dataset. (L) Hsa-miR-26a-3p expression level in 178 alive and 59 dead LIHC patients from GSE6857 dataset.